Interplay of spin and charge dynamics in $Sr_{14-x}Ca_xCu_{24}O_{41}$

V. Kataev,[1,*] K.-Y. Choi,[1] M. Grüninger,[1] U. Ammerahl,[1,2] B. Büchner,[1,†] A. Freimuth,[1] and A. Revcolevschi[2]
[1]*II. Physikalisches Institut, Universität zu Köln, D-50937 Köln, Germany*
[2]*Laboratoire de Chimie des Solides, Université Paris-Sud, 91405 Orsay Cédex, France*
(Received 22 December 2000; published 23 August 2001)

In single crystals of intrinsically hole-doped $Sr_{14-x}Ca_xCu_{24}O_{41}$ a strong electron spin resonance (ESR) signal has been observed and studied as a function of temperature and Ca concentration ($x=0-12$). Since the spin ladders show a large spin gap of about 400–500 K, the dominant contribution to the ESR signal below 300 K is attributed to the CuO_2 spin-1/2 chains. For all values of x the data reveal a remarkable influence of the hole dynamics on the Cu-spin relaxation. This enables us to identify the onset of charge order in the chains for $x=0$ and 2 at 200 and 170 K, respectively. A further increase of x rapidly destroys the charge ordered state. A transition to an antiferromagnetically ordered state is observed at 2.5 K for $x=12$. However, the ESR signal shows critical broadening already for $x\geqslant 8$ at low temperatures, which indicates the development of magnetic order for values of x smaller than 12. For comparison we show ESR data of $La_1Sr_{13}Cu_{24}O_{41}$ and $La_2Ca_{12}Cu_{24}O_{41}$, in which the hole concentration is reduced. The whole set of ESR data can be understood in terms of a transfer of only a *small* amount of holes from the chains to the ladders with increasing x in $Sr_{14-x}Ca_xCu_{24}O_{41}$ and a simultaneous crossover from independent dimers to antiferromagnetically coupled chains, which order at low temperatures due to weak interchain interactions.

DOI: 10.1103/PhysRevB.64.104422 PACS number(s): 76.30.−v, 71.27.+a, 71.70.Gm, 75.40.Gb

I. INTRODUCTION

The interesting interplay of spin and charge degrees of freedom in the complex one-dimensional transition-metal oxide $Sr_{14-x}Ca_xCu_{24}O_{41}$ has recently attracted much attention. Depending on the Ca concentration, one observes magnetic and charge ordering phenomena, metallic conductivity, and superconductivity under external pressure.[1] The compound possesses a complex layered structure of alternating Cu_2O_3 and CuO_2 sheets which are separated by (Sr,Ca) layers.[2] The Cu_2O_3 layers consist of two-leg spin-1/2 ladders which are built by corner-sharing Cu–O plaquettes. Within the ladders the ~180° Cu–O–Cu bonds give rise to a strong antiferromagnetic (AF) superexchange coupling between the Cu spins, both along the legs and the rungs.[3–5] Neighboring ladders can be considered as magnetically decoupled because they are connected by 90° Cu–O–Cu bonds, which cause a weak and frustrated interladder exchange interaction. The CuO_2 planes are composed of spin-1/2 chains of *edge*-sharing Cu–O–plaquettes, i.e., along the chains the Cu spins are coupled via nearly 90° Cu–O–Cu bonds.

Independent of the Ca concentration the average Cu valence in $Sr_{14-x}Ca_xCu_{24}O_{41}$ is 2.25, i.e., the compound is intrinsically doped with six holes per formula unit (f.u.). However, the electronic and magnetic properties depend strongly on the Ca content. We first focus on Ca-free $Sr_{14}Cu_{24}O_{41}$. A calculation of the Madelung potentials suggests[6] that for $x=0$ most of these six holes are localized in the chains due to their larger electronegativity, resulting in a hole concentration of about 6/10 per Cu site in the chains. Recent polarization-dependent x-ray absorption data[7] indicate $n=0.8$ holes per formula unit in the ladders for $x=0$. As predicted on theoretical grounds,[1] the spin ladders of $Sr_{14}Cu_{24}O_{41}$ have a singlet ground state with a spin gap of about 400–500 K.[8–10] Surprisingly, also the spin chains show a singlet ground state, in this case with a spin gap of about 130 K.[10–13] The occurrence of this nonmagnetic ground state is related to the large hole concentration in the chains and to the localization of these holes below about 200 K.[4,5,12–14] The building units of the nonmagnetic ground state are spin dimers[11,13] which are formed between those *next*-nearest-neighbor Cu spins[12] that are separated by a localized Zhang-Rice singlet,[15] i.e., by a site occupied by a localized hole [see Fig. 1(a)]. Neutron diffraction[4,5] as well as x-ray scattering experiments on $Sr_{14}Cu_{24}O_{41}$ (Ref. 14) reveal a periodic spacing of spin dimers together with an additional

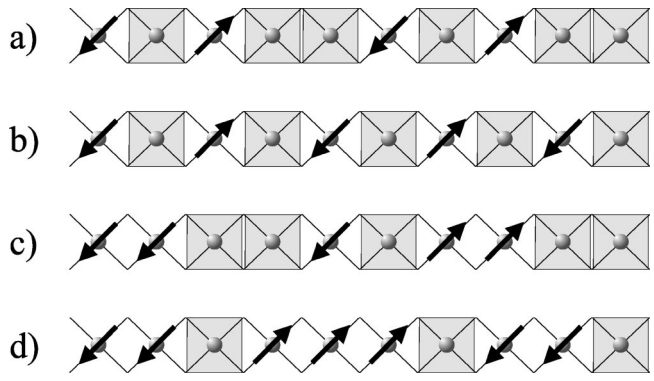

FIG. 1. Illustration of possible spin structures for different doping levels of the CuO_2 chains. Circles indicate Cu sites, the ten sites represent one formula unit of the chains. The gray squares denote Zhang-Rice singlets. (a) The charge-ordered dimerized state with six holes per formula unit. Dimers are formed between next-nearest neighbors, two dimers are separated by two Zhang-Rice singlets. (b) A homogeneous antiferromagnetic chain can be formed with five holes per formula unit. (c) A disordered arrangement of holes combines AF next-nearest-neighbor couplings with ferromagnetic nearest-neighbor couplings. (d) A further decrease of the hole count results in short ferromagnetic chain fragments that are coupled antiferromagnetically to each other.

structural periodicity, which indicates charge order in the chains. This is corroborated by an anomaly in thermal expansion data.[12] The localization of the holes is confirmed by the semiconducting behavior of the electrical resistivity.[13] Moreover, the resistivity data of $Sr_{14}Cu_{24}O_{41}$ reveal a peak of $d\ln(\rho)/d(1/T)$, i.e., a change of the effective activation energy at about 250 K which also points towards the onset of charge order in the chains.[13] Remarkably, the isotropic intradimer exchange interaction between next-nearest neighbors $\mathcal{H}_{\rm iso}=J_{nnn}\Sigma_i \boldsymbol{S}_i\boldsymbol{S}_{i+2}$ differs quite substantially from the usual nearest-neighbor coupling in a chain with 90° Cu-O-Cu bonds. The latter is weak and ferromagnetic, whereas the intradimer exchange J_{nnn} is antiferromagnetic and much larger, $J_{nnn}\approx 130$ K,[13,16] which can be deduced from the magnitude of the spin gap. Interdimer couplings amount to about 10% of J_{nnn} both along and perpendicular to the chains.[3–5]

Isovalent substitution of the smaller Ca^{2+} for Sr^{2+} strongly changes the electronic properties of $Sr_{14-x}Ca_xCu_{24}O_{41}$. With increasing Ca content the system becomes more conducting.[13,17] Additional application of high external pressure leads to a metal-insulator transition and finally to superconductivity with $T_c\approx 10$–12 K.[18,19] It is generally assumed that the chemical pressure induced by Ca substitution leads to a transfer of holes from the chains to the ladders, which can be attributed to the change of the electrostatic potentials.[6] In this scenario the ladders provide the conducting channel, and neither metallic conductivity nor superconductivity can be attributed to the chains. The occurrence of superconductivity in even-leg ladders had been predicted theoretically.[20] Experimentally, the precise extent of the hole transfer is currently under debate. A substantial increase of the hole count in the ladders from $n=1$ holes per formula unit for $x=0$ to $n=2.8$ for $x=12$ was deduced from optical conductivity data[21] and from $n=2$ for $x=6$ to $n=3.5$ for $x=11.5$ from NMR.[8] On the other hand, recent polarization-dependent x-ray absorption data[7] indicate $n=0.8$ holes per formula unit in the ladders for $x=0$ and only a marginal increase to $n=1.1$ for $x=12$. With increasing x the x-ray data also reveal an increasing occupancy of those oxygen orbitals in the ladders that are oriented along the a axis, i.e., parallel to the rungs,[7] thus suggesting a more ''two-dimensional'' character of the ladders. However, the chemical pressure induced with increasing x also results in a larger overlap of Cu d and oxygen p orbitals in the chain layers, possibly making them more two-dimensional and therefore more conducting too, as discussed in Ref. 13.

From the point of view of magnetic measurements the issue of the hole transfer appears to be controversial, too. In particular, since the spin gaps in both chains and ladders are expected to be sensitive to the hole doping of the respective subsystems, one might hope to shed some light on the redistribution of holes by studying the influence of Ca substitution on the two gaps. As far as the ladders are concerned, NMR data[8,9] indicate a suppression of the spin gap upon Ca substitution, thus suggesting an appreciable hole transfer to the ladders. However, recent neutron scattering experiments reveal no doping dependence of the ladder spin gap.[22] NMR measurements[9] of $1/T_1$ suggest that the dimer spin gap of the chains is not affected by Ca substitution, indicating an appreciable amount of holes in the chains even at high Ca concentration. Carter *et al.*[13] analyzed their static susceptibility data of polycrystalline samples in terms of a dimerized state up to $x=10$ and found no dependence of the dimer spin gap on x. However, this interpretation requires a drastic increase of the paramagnetic background χ_0 from about 1×10^{-4} emu/mole Cu for $x=0$ to about 13×10^{-4} emu/mole Cu for $x=10$. Moreover, thermal expansion data of $Sr_{14-x}Ca_xCu_{24}O_{41}$ indicate that the occurrence of a rather large spin gap is closely related to the presence of charge order, which is suppressed with increasing x.[12] Charge order is *not* seen in the resistivity curves of $Sr_{14-x}Ca_xCu_{24}O_{41}$ for large x.[13] Recently, Ammerahl *et al.*[23] have shown that a consistent description of the susceptibility and of magnetization data can be obtained for $x=12$ in terms of antiferromagnetically coupled *homogeneous* chains, where the dominant coupling is still between next-nearest neighbors [see Fig. 1(b)]. In this scenario, the gap is obviously zero for $x=12$. Note that for a given coupling J_{nnn} the temperature at which the susceptibility has a maximum is rather similar for independent dimers and an AF chain.[24] Remarkably, in samples with $x\geqslant 11.5$ antiferromagnetic order has been observed in the chain subsystem at $T\gtrsim 2$ K (Refs. 26–28). In the scenario of AF chains the occurrence of long-range order is naturally explained by weak interchain interactions.[23]

Obviously, the interplay of spin and charge degrees of freedom plays a crucial role in determining the magnetic and transport properties of $Sr_{14-x}Ca_xCu_{24}O_{41}$. This compound seems to offer a unique playground where one can switch between very different magnetic states by controlling the hole concentration and the steric parameters.

Recently, a well defined electron spin resonance (ESR) response from the Cu spins in $Sr_{14}Cu_{24}O_{41}$ has been reported.[16,29] Due to the large spin gap of the ladders, the magnetic properties below 300 K and hence also the ESR signal are entirely determined by the chains. Therefore ESR can be used as a powerful tool to study the strength and anisotropy of inter- and intrachain magnetic interactions, as well as the spin and charge dynamics in the chains. In a recent paper[30] we have reported the ESR response of $La_{14-y}Ca_yCu_{24}O_{41}$. There, we have found an unusually large, temperature-independent linewidth $\Delta H\approx 1500$ Oe of the Cu^{2+} ESR signal, which has been shown to reflect the large anisotropy of the ferromagnetic nearest-neighbor superexchange in the nearly 90° Cu-O-Cu bonding geometry of this compound. In the present work, we report on the results of an extensive ESR study of single crystals of $Sr_{14-x}Ca_xCu_{24}O_{41}$ with seven different Ca concentrations between $x=0$ and 12. We investigate various aspects of the interplay between magnetism, hole mobility, and structural features of the CuO_2 chains: (i) Our data reveal a remarkable influence of the hole dynamics on the Cu-spin relaxation. In the charge ordered state the Cu-spin relaxation freezes out, giving rise to a very narrow and temperature-independent ESR line for $x=0$ and 2 at low temperatures. A strong increase of the linewidth ΔH above a certain characteristic temperature T^* indicates the melting of charge order at T^*. (ii) T^* rapidly decreases from about 200 K for $x=0$ to

~ 80 K for $x=5$. Moreover, for $x=5$ the linewidth ΔH at $T=50$ K$<T^*$ is about a factor of 4 larger than for $x=0$ or 2. Both observations indicate that the charge ordered state is rapidly destroyed by substituting Ca for Sr, resulting in the destabilization of the spin dimerized state. (iii) For $x \geqslant 8$ we find critical broadening of the ESR line at low temperatures which signals a transformation from the nonmagnetic spin dimerized ground state to a magnetically ordered state with increasing Ca content. A well-defined transition to an antiferromagnetically long-range ordered state is observed for $x=12$ at 2.5 K, in agreement with previous studies.[26–28] (iv) For all values of x the existence of a strong temperature-dependent contribution to the linewidth associated with the charge dynamics suggests the presence of a substantial amount of mobile holes in the chains, even at large values of Ca doping. (v) The temperature-independent contribution to the linewidth is at least a factor of 3 smaller in $Sr_{14-x}Ca_xCu_{24}O_{41}$ than in $La_{14-y}Ca_yCu_{24}O_{41}$ for all values of x. The very broad linewidth of the latter system reflects the large anisotropy of the nearest-neighbor exchange, which becomes dominant if the hole concentration in the chains is *significantly* reduced. The much narrower line observed in $Sr_{14-x}Ca_xCu_{24}O_{41}$ demonstrates that the dominant coupling is the one between *next-nearest* neighbors for $0 \leqslant x \leqslant 12$. This is in agreement with a transfer of only a *small* amount of holes from the chains to the ladders.

II. EXPERIMENT

Single crystals of $Sr_{14-x-y}Ca_xLa_yCu_{24}O_{41}$ were grown in an image furnace using the traveling solvent floating zone method. All samples were thoroughly characterized by means of electron microscopy, energy-dispersive x-ray analysis (EDX), x-ray and neutron diffraction (for details, see Ref. 31). For the ESR measurements, small specimens with masses of $m \sim 6-30$ mg were cleaved from large single domain crystals. For the present work we have studied $La_1Sr_{13}Cu_{24}O_{41}$, $La_2Ca_{12}Cu_{24}O_{41}$, and $Sr_{14-x}Ca_xCu_{24}O_{41}$ with $x=0$, 2, 5, 8, 9, 11, and 12.

ESR measurements were performed in the *X*-band frequency range ($\nu \approx 9.47$ GHz). A helium gas flow cryostat inserted into the microwave cavity was used to achieve temperatures from 300 K down to 1.9 K. In order to obtain the ESR intensity in absolute units and to minimize the uncertainty in its temperature dependence, the intensity of the measured signal was calibrated against the intensity of a so-called ''witness'' sample (a standard reference single crystal $Al_2O_3+0.03\%$ Cr^{3+}). The ''witness'' sample was attached to the wall inside the cavity, which is kept at a constant temperature of 300 K. In this way one can eliminate possible changes of the quality factor of the resonance cavity due to temperature-dependent microwave losses in the sample, as well as other factors which affect the sensitivity of the spectrometer.

The magnetic susceptibility $\chi_{\rm stat}$ was measured in the temperature range from 4.2 to 300 K with a commercial superconducting quantum interference device (SQUID) magnetometer. A field of 1 T was applied along the *c* axis of the samples (0.1 T in the case of $x=11$). We note that according to measurements of the static magnetization performed in Ref. 23 $\chi_{\rm stat}$ is field independent for $T \gtrsim 25$ K and $0<\mathbf{H} \leqslant 14$ T.

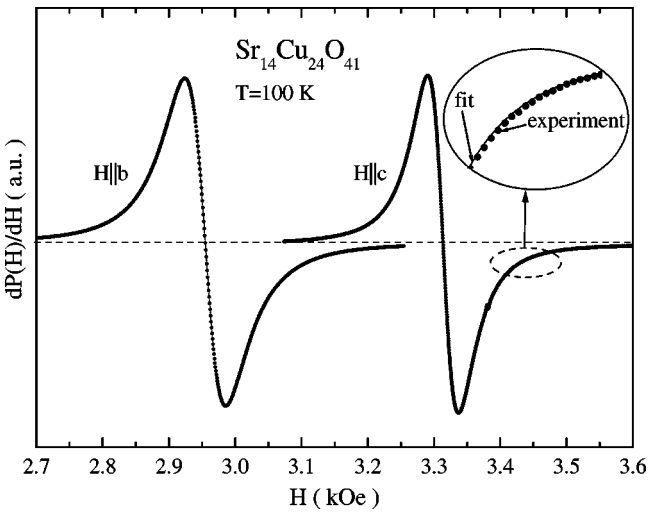

FIG. 2. ESR spectra of $Sr_{14}Cu_{24}O_{41}$ at $T=100$ K for $\mathbf{H} \| b$ and $\mathbf{H} \| c$ (dots). Note that the spectrometer measures the field derivative of the absorbed microwave power, $dP(H)/dH$. The solid lines denote Lorentzian fits. Concerning the Lorentzian line shape and the anisotropy of both the resonance field and the linewidth, these spectra are representative for the $Sr_{14-x-y}Ca_xLa_yCu_{24}O_{41}$ system.

III. RESULTS AND DISCUSSION

The ESR spectrum of $Sr_{14-x-y}Ca_xLa_yCu_{24}O_{41}$ consists of a single line. Representative examples of the resonance signal for $\mathbf{H} \| b$ (normal to the planes of chains and ladders) and $\mathbf{H} \| c$ (parallel to both chains and ladders) are shown in Fig. 2. Note that the spectrometer measures the field derivative of the absorbed microwave power, $dP(H)/dH$. In the entire temperature range of the measurements, the ESR signal of all samples that we have studied can be fitted very well by a Lorentzian line profile (see Fig. 2):

$$f(H) = -\frac{16ah}{(3+h^2)^2}, \quad h = \frac{2(H-H_{res})}{\Delta H}. \tag{1}$$

Here, a, $H_{\rm res}$, and ΔH denote the amplitude, the resonance field, and the width of the Lorentzian absorption derivative, respectively.

A. *g*-factors

For $T>10$ K the resonance field $H_{\rm res}$ is practically constant for all samples studied and depends only on the orientation of the magnetic field **H** with respect to the crystallographic axes. The corresponding *g*-factor $g=h\nu/\mu_B H_{\rm res}$ follows $g^2(\theta)=g_b^2\cos^2(\theta)+g_c^2\sin^2(\theta)$, where θ denotes the angle between the external magnetic field and the *b* axis. Our results for the principal *g*-factors g_b and g_c are summarized in Table I. The experimental error bars are larger for $\mathbf{H} \| b$ because also the ESR linewidth ΔH is larger for this orientation (see Fig. 2). These *g*-factors are typical for the ESR

TABLE I. Principal g-factors of the crystals studied.

Sample	g_b	g_c
$Sr_{14-x}Ca_xCu_{24}O_{41}$		
$x=0$-5	2.28 ± 0.03	2.04 ± 0.02
$x=8$	2.29 ± 0.04	2.03 ± 0.03
$x=9$-12	2.32 ± 0.04	2.03 ± 0.03
$La_1Sr_{13}Cu_{24}O_{41}$	2.33 ± 0.05	2.07 ± 0.03
$La_2Ca_{12}Cu_{24}O_{41}$	2.30 ± 0.05	2.02 ± 0.03

response of Cu^{2+} ions in a $d_{x^2-y^2}$ ground state in a crystal field of axial symmetry.[32] From this point of view, the ESR signal could in principle originate from both chains and ladders, since the Cu ions in both subsystems are fourfold oxygen coordinated in the ac plane with the b axis as the axial symmetry axis. However, due to the large spin gap the contribution of the ladders to the magnetic properties is expected to be very small for $T\leqslant 300$ K, and the ESR response must be attributed to the Cu ions in the chains (see below).

For Cu^{2+} ions in a $3d^9$ configuration in a crystal field of tetragonal symmetry the g-factors are usually estimated as[32]

$$g_c=2-\frac{2\lambda}{\Delta_{yz,zx}},\quad g_b=2-\frac{8\lambda}{\Delta_{xy}}, \tag{2}$$

where, e.g., Δ_{xy} is the crystal-field splitting between the $d_{x^2-y^2}$ ground state and the d_{xy} level, and λ denotes the spin-orbit coupling with $\lambda\approx-100$ meV (Ref. 32) for a free Cu^{2+} ion. Using the average values $2-g_b\approx0.3$ and $2-g_c\approx0.04$ from Table I, we find $\Delta_{xy}\approx2.7$ eV and $\Delta_{yz,zx}\approx5$ eV. Note that the Cu ions in the chains do not have an apical oxygen and that the chain layers are sandwiched between positively charged (Sr,Ca,La) layers, which may shift in particular the d_{yz} and d_{zx} levels to high energies. However, this naive estimate of the crystal-field levels should be taken with some reservation, since Eq. (2) is based on first-order perturbation theory and assumes a purely ionic bonding character. It neither accounts for a possible anisotropy of spin-orbit coupling in a low-symmetry coordination nor for a possible reduction of its magnitude due to covalency effects.[32]

B. ESR intensity and static susceptibility

The integrated intensity I of the ESR spectrum is determined by the susceptibility χ_{ESR}^{spin} of the spins participating in the resonance.[32] For the Lorentzian line shape described by Eq. (1) one finds $I=3.63a(\Delta H)^2$. The calibration of the ESR intensity I against the ''witness'' sample with known χ_{ESR}^{spin} allows us thus to determine the ESR spin susceptibility $\chi_{ESR}^{spin}(T)$ of $Sr_{14-x-y}Ca_xLa_yCu_{24}O_{41}$.

In Fig. 3 we plot χ_{ESR}^{spin} (top panel) and the static susceptibility χ_{stat} (bottom panel) of $Sr_{14-x}Ca_xCu_{24}O_{41}$ for various x. Obviously, the temperature dependence of the two data sets is qualitatively similar, although χ_{ESR}^{spin} represents only the susceptibility of those spins which participate in the resonance. In Ca-free $Sr_{14}Cu_{24}O_{41}$ the susceptibility increases moderately with decreasing temperature, passes through a broad maximum around 100 K and then rapidly decreases and reaches a minimum at $\sim$25 K. With increasing Ca content x, this minimum is rapidly smeared out in both data sets. Also the strong $1/T$-like upturn at lower temperatures is observed in both χ_{stat} and χ_{ESR}^{spin} for all values of x. However, there are also certain noticeable discrepancies: χ_{ESR}^{spin} tends to be somewhat smaller than $\chi_{stat}(T)$; in $Sr_{14}Cu_{24}O_{41}$ the maximum of $\chi_{stat}(T)$ occurs at $\sim$77 K, whereas χ_{ESR}^{spin} peaks at $\sim$87 K; and the ESR results for $x=8$ and, in particular, $x=12$ show a real minimum at 25 K, which is much less pronounced in χ_{stat}.

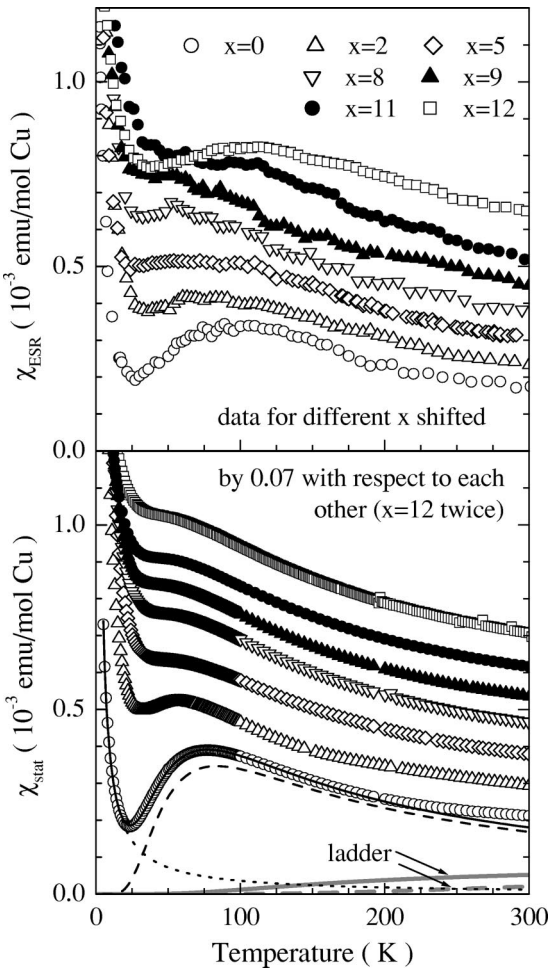

FIG. 3. Temperature dependence of the ESR response $\chi_{ESR}^{spin}(T)$ (top panel) and of the static magnetic susceptibility $\chi_{stat}(T)$ (lower panel) of $Sr_{14-x}Ca_xCu_{24}O_{41}$ for various x. The magnetic field has been applied along the c axis. The absolute scale refers to the $x=0$ data, all other curves are shifted by 0.07 with respect to each other (the $x=12$ data have been shifted twice). Solid line: Fit of χ_{stat} below 200 K for $x=0$ using a dimer contribution (dashed) and a Curie term (dotted). Grey lines: estimate of the ladder contribution for $J_{leg}=1500$ K and $J_{leg}/J_{rung}=0.5$ (solid) and 1 (dashed) according to the quantum Monte Carlo results of Ref. 34.

It is well established that the dominant contribution to χ_{stat} originates from the chains.[13,16,17] The similarity between χ_{stat} and χ_{ESR}^{spin} suggests that (i) also the ESR signal can be attributed to the chain site Cu ions, and that (ii) most of the spins contributing to the bulk static susceptibility also par-

ticipate in the magnetic resonance. The strong upturn of $\chi_{\rm stat}$ for $T<25$ K is due to quasifree spins. The origin of these quasifree spins is not precisely known, but it is very likely that they have to be identified with some short spin-chain fragments. These may arise due to a nonuniform distribution of holes in the chains. Note that perfect charge order with two adjacent dimers separated by two Zhang-Rice singlets requires six holes in the chains per formula unit [see Fig. 1(a)], a condition most probably never fulfilled. At low temperatures, the magnetic susceptibility of such fragments resembles that of free spins, i.e., it is expected to diverge as $1/T$.[33]

For small values of x, the total static magnetic susceptibility $\chi_{\rm stat}$ is well described by the independent spin-dimer model with a spin gap of about 130 K between the nonmagnetic singlet ground state and the excited spin triplet state.[12,13,16,17] We approximate the experimental data for $x=0$ by summing a Curie-Weiss term $\chi_{\rm Curie}$ and a contribution of independent spin dimers $\chi_{\rm dimer}$ (Ref. 23),

$$\chi_{\rm stat}(T)=\chi_{\rm Curie}+\chi_{\rm dimer} =\frac{N_A g^2\mu_B^2}{24\,k_B}\left[\frac{N_{\rm free}}{4(T-T_c)}+\frac{2N_{\rm dimer}}{T[3+\exp(J_{nnn}/k_BT)]}\right], \tag{3}$$

where $N_{\rm free}$ and $N_{\rm dimer}$ denote the density of quasifree spins and of dimers, respectively, J_{nnn} is the intradimer exchange coupling between next-nearest-neighbor spins, and T_c labels the Curie-Weiss temperature. A spin of $S=1/2$ has been assumed.

We neglect the temperature-independent contributions to the static susceptibility due to the van Vleck paramagnetism of Cu^{2+} ions $\chi_{\rm vV}^{Cu}$ and the core diamagnetism $\chi_{\rm dia}^{\rm core}$, since both are expected to be small and practically compensating each other. An estimate of $\chi_{\rm dia}^{\rm core}$ as a sum of the respective contributions from all ions comprising the lattice gives a value of the order of -10^{-5} emu/mole Cu. The van Vleck susceptibility is set by the crystal-field splitting of the orbital states of Cu^{2+},

$$\chi_{{\rm vV},c}^{Cu}=2N_A\mu_B^2/\Delta_{yz,zx}, \quad \chi_{{\rm vV},b}^{Cu}=8N_A\mu_B^2/\Delta_{xy}. \tag{4}$$

With a crystal-field splitting of a few eV as derived from the g-factors, a rough estimate gives $\chi_{\rm vV}^{Cu}\sim 10^{-5}$ emu/mole Cu.

Obviously, the description of the susceptibility in terms of independent dimers should work particularly well in the charge ordered state. According to our analysis of the ESR linewidth (see below) the charge order in $Sr_{14}Cu_{24}O_{41}$ sets in at about 200 K. Therefore we have restricted the fit of $\chi_{\rm stat}$ of $Sr_{14}Cu_{24}O_{41}$ to temperatures below 200 K. Indeed, in this temperature range the fit by Eq. (3) with $N_{\rm free}=0.22$ per f.u., $2N_{\rm dimer}=3.56$ per f.u., $T_c=0.16$ K, and $J_{nnn}=134$ K approximates the experimental data very well (solid line in Fig. 3, the two contributions $\chi_{\rm Curie}$ and $\chi_{\rm dimer}$ correspond to the dotted and dashed lines, respectively).

At higher temperatures, the experimental data fall off much slower than the fit. This discrepancy is frequently attributed to the ladder contribution $\chi_{\rm ladder}$. The dominant parameter for the absolute value of $\chi_{\rm ladder}$ at 300 K is not the ladder gap of about 400 K, but the strong antiferromagnetic superexchange coupling.[34] Since the precise exchange parameters of the ladders $J_{\rm leg}$ and $J_{\rm rung}$ are currently under debate,[35] the estimate of the ladder contribution to the total static susceptibility of $Sr_{14}Cu_{24}O_{41}$ is rather uncertain. The two gray lines in the bottom panel of Fig. 3 denote rough estimates of $\chi_{\rm ladder}$ based on the quantum Monte Carlo results of Johnston and collaborators,[34] using $J_{\rm leg}=1500$ K and $J_{\rm rung}/J_{\rm leg}=1/2$ (solid gray line) and $J_{\rm rung}/J_{\rm leg}=1$ (dashed).

A thorough discussion of $\chi_{\rm stat}$ for larger values of x is given in Ref. 23. Here, we only cite the main results: the model of noninteracting dimers of Eq. (3) describes the experimental data very well only for small values of x at low temperatures, i.e., in the charge ordered state. Mobile charges in the chains will cause deviations from the dimer model, e.g., by producing a broad distribution of the strength of the intradimer coupling J_{nnn} (see also Ref. 12). For $x=12$ the data agree nicely with the theoretical results for a homogeneous antiferromagnetic chain of Klümper.[37] The temperature $T_{\rm max}$ at which the static susceptibility acquires a local maximum decreases with increasing x (see Fig. 3). Independent of the model used[24] the reduction of $T_{\rm max}$ indicates that the next-nearest-neighbor coupling $J_{nnn}=134$ K for $x=0$ is reduced with increasing x. Assuming an antiferromagnetic chain, the $x=12$ data yield $J=103$ K.[23] Note that one can easily construct a homogeneous, antiferromagnetically coupled chain with five holes per formula unit: Due to the Coulomb repulsion, the holes will occupy next-nearest neighbor sites and give rise to a strong antiferromagnetic coupling between the spins [see Fig. 1(b)].

The ESR results show further indications for a smooth transition from spin dimers to a uniform spin chain with increasing Ca concentration, which will be discussed in the following section.

C. Linewidth

1. Dimers and charge dynamics

Compared to the intensity $I(T)$, i.e., $\chi_{\rm ESR}^{\rm spin}$, the linewidth ΔH of the ESR spectrum and the resonance field $H_{\rm res}$ can be determined with a significantly higher accuracy. Similar to the case of the resonance field $H_{\rm res}$ discussed in connection with the g-factors, the width ΔH of the resonance line is anisotropic. For a fixed temperature, ΔH is proportional to $(1+\cos^2\theta)$, where θ is the angle between the magnetic field $\mathbf{H}$ and the b axis. Since the determination of the parameters is more accurate for narrow ESR lines, we will concentrate in the following on the case of $\mathbf{H}\|c$. The temperature dependence $\Delta H(T)$ is shown in Fig. 4 for all crystals studied. In the following we first discuss the high-temperature regime $T\gtrsim 30$ K and then the low-temperature regime $T\lesssim 30$ K where the Curie-contribution dominates the susceptibility (dotted line in Fig. 3).

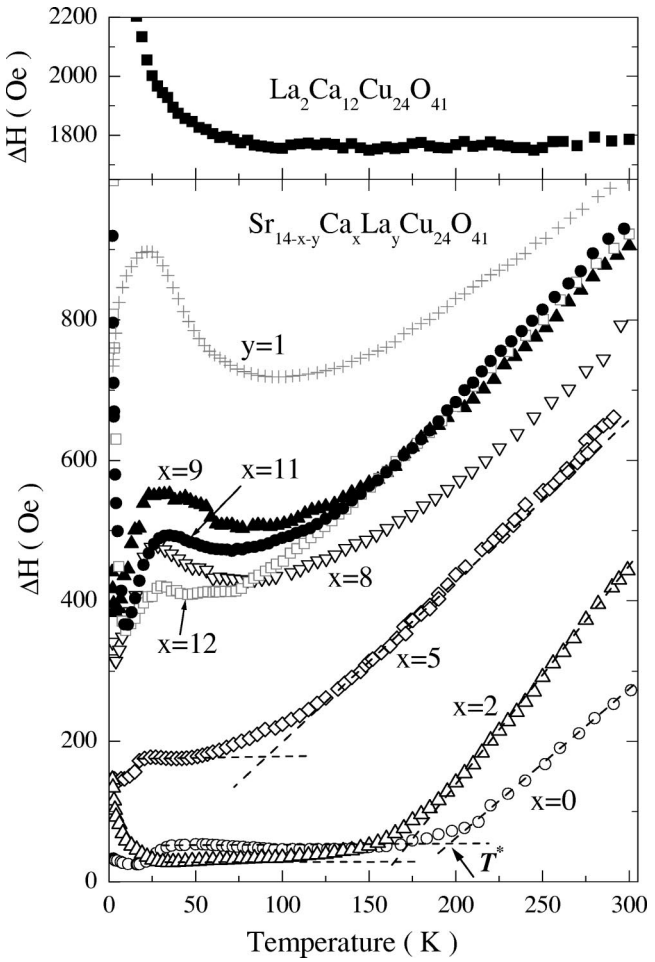

FIG. 4. Bottom panel: temperature dependence of the linewidth $\Delta H(T)$ of $Sr_{14-x}Ca_xCu_{24}O_{41}$ for various x. The topmost curve shows data for $La_1Sr_{13}Cu_{24}O_{41}$. The magnetic field has been applied along the c axis of the crystals. The dashed lines denote the constant and linear contributions to $\Delta H(T)$ as defined by Eq. (5). We define T^* as the crossing point of the dashed lines. Top panel: same for $La_2Ca_{12}Cu_{24}O_{41}$.

In $Sr_{14}Cu_{24}O_{41}$ the width ΔH is almost constant between 30 and $\sim$180 K, but for higher temperatures it increases rapidly and approximately linearly with temperature. We approximate $\Delta H(T)$ phenomenologically as

$$\Delta H(T) = \Delta H_0 + \Delta H^*(T) \tag{5}$$

with $\Delta H^*(T) = \text{const} \times (T - T^*)$ for $T > T^*$, and $\Delta H^*(T) = 0$ for $T < T^*$, where T^* is the characteristic temperature of the crossover between the two distinctly different regimes, as defined in Fig. 4.

In concentrated paramagnetic systems a constant contribution ΔH_0 to the ESR linewidth is determined mainly by (i) the isotropic exchange narrowing effect, (ii) inhomogeneities (both magnetic and structural), and (iii) anisotropic spin-spin interactions like, e.g., dipole-dipole interactions and anisotropic exchange.[32,38] The second term $\Delta H^*(T)$ accounts for other, *temperature-dependent* spin-relaxation mechanisms. The experimental result that this contribution arises only above T^*—at least for $x=0$ and 2, and with less confidence also for $x=5$—indicates a characteristic energy scale for the appearance of a new degree of freedom in the chains.

We associate this with the charge dynamics in the chains, i.e., with the melting of charge order at T^*. Since the spins in a dimer are coupled via a localized Zhang-Rice singlet, an increase of hole mobility will reduce the dimer lifetime, shorten its spin relaxation time, and broaden the ESR linewidth. Hence the constant width ΔH_0 of the signal below T^* corresponds to the localization of the charge carriers, and the strong increase of ΔH above T^* reflects the thermally activated hole mobility.

Both the crossover temperature T^* and ΔH_0 turn out to be very sensitive to Ca substitution (see Fig. 4). Whereas T^* amounts to 200 K for "pure" $Sr_{14}Cu_{24}O_{41}$, it decreases to 170 K for $x=2$ and to 80 K for $x=5$. This rapid decrease of T^* upon Ca substitution clearly indicates an increasing instability of the charge ordered state in the chains. For still larger values of x it is not possible to define a T^* below which ΔH is constant, i.e., there is no signature of charge order.

Our interpretation of $T^*(x)$ as the charge ordering temperature is in agreement with results based on other techniques. In $Sr_{14}Cu_{24}O_{41}$ neutron scattering data[4,5] reveal a quasi-2D *ordering* of holes in the chains below $\sim$150 K,[4] whereas in x-ray measurements the satellite peaks indicating charge order disappear close to 300 K.[14] Detailed NMR/nuclear quadrupole resonance (NQR) studies reveal a static distribution of holes below 200 K for $x=0$ (Ref. 43). Resistivity data[13,23] show a peak of the derivative $d\ln(\rho)/d(1/T)$, i.e., a change of the effective activation energy at about 250 K for $x=0$, 180 K for $x=2$, and 120 K for $x=4$, which has been discussed in terms of charge order in the chains.[13] For larger values of x this peak is much less pronounced, but one can still observe a shallow maximum at about 80 K.[13] The anomaly in thermal expansion data[12] gives 180 K for $x=2$, 80 K for $x=5$, and 50 K for $x=8$, and the size of the anomaly is drastically suppressed with increasing x.

For small values of x we have attributed the increasing linewidth above T^* to the enhanced hole mobility: the hopping of holes along the chains causes spin flips and therefore a broadening of the ESR line. It is straightforward to use the same interpretation for the increase of ΔH for large values of x. The fact that hole mobility shortens the relaxation time of copper spins does not depend on whether the zero-temperature ground state is dimerized or not. Remarkably, the slope of the increasing linewidth $\Delta H^*(T)$ is approximately the same for all values of x, suggesting the presence of a substantial amount of mobile holes in the chains even at large Ca concentration. We note that an x-independent slope of $\Delta H^*(T)$ is compatible with a certain decrease of the hole concentration in the chains, if this is compensated by a decrease of the activation energy for charge motion. In this context the ΔH data of $La_1Sr_{13}Cu_{24}O_{41}$ ("+"-signs in Fig. 4) are of particular interest. In this compound the hole count is reduced from six to five per formula unit by substitution of trivalent La ions. In the x-ray absorption measurements of Ref. 7 all holes reside in the chains in all samples with reduced hole count. Remarkably, the slope of $\Delta H^*(T)$

observed at high temperatures in $La_1Sr_{13}Cu_{24}O_{41}$ is very similar to the results of $Sr_{14-x}Ca_xCu_{24}O_{41}$ (see Fig. 4). The data of $La_2Ca_{12}Cu_{24}O_{41}$ (top panel of Fig. 4, note the different scale) with nominally four holes per formula unit clearly demonstrate that a further decrease of the hole concentration results in a considerable reduction of the slope of $\Delta H^*(T)$ and in a very much larger linewidth at all temperatures.

The temperature-independent contribution to the ESR linewidth ΔH_0 [see Eq. 5] strongly depends on x also. It increases rapidly from ~ 50 Oe for $x=0$ to ~ 500 Oe for $x=9$, and then decreases again down to 400 Oe for $x=12$. Note that ΔH_0 amounts to about 700 Oe in $La_1Sr_{13}Cu_{24}O_{41}$ and about 1800 Oe in $La_2Ca_{12}Cu_{24}O_{41}$. All three different effects stated above (i.e., the exchange narrowing effect, inhomogeneous broadening, and anisotropic spin-spin interactions) which determine a temperature-independent linewidth may possibly contribute to a dependence of ΔH_0 on the Ca concentration.

(i) A reduction of the effective exchange coupling between the resonating spins gives rise to a reduced exchange narrowing and thereby to an increase of ΔH_0. An analysis of the susceptibility data discussed above (see also Refs. 12 and 23) reveals a reduction of J_{nnn} by about 20–25% from $x=0$ to $x=12$.

(ii) Inhomogeneous contributions $\Delta H_{\rm struc}$ to ΔH_0 may arise due to, e.g., random structural distortions of Cu-O plaquettes induced locally by substitution of Sr^{2+} for the smaller Ca^{2+} ions. This contribution should vary approximately as $(14-x)x$, i.e., it should vanish for $x=0$ or 14. Indeed, we observe a small reduction of ΔH_0 for $x>9$ from 500 to 400 Oe. Together with the small width for $x=2$ this allows us to give an upper limit of $\Delta H_{\rm struc}$ of about 150 Oe. Note that the Sr-Ca sublattice is incommensurate with the chains,[2] resulting in an inhomogeneous contribution even for $x=0$, where ΔH_0 is very small. This once more indicates the limited influence of structural disorder. Probably more important is the possible role of magnetic disorder. The magnetic Cu sites in the chains are equivalent only in the charge ordered dimerized state [compare, e.g., Fig. 1(a) with Figs. 1(c) and (d)]. In the absence of charge order the spins will be exposed to locally different exchange or dipolar fields, which gives rise to an enhanced linewidth. However, these inhomogeneous contributions definitely do not dominate ΔH_0 since the ESR spectrum remains a single Lorentzian line without a significant distortion or deviations towards, e.g., a Gaussian line shape.

(iii) An increase of the *anisotropic* contribution to superexchange will cause a growing linewidth.[32] In a recent paper[30] we have shown that the very broad ESR line observed in $La_{14-x}Ca_xCu_{24}O_{41}$ (see, e.g., top panel of Fig. 4) can be attributed to the unusually large anisotropy of the *nearest-neighbor* exchange, which becomes dominant for low hole concentrations. The *isotropic* Heisenberg superexchange interaction between *nearest-neighbor* Cu spins $\mathcal{H}_{\rm iso}=J_{\rm iso}\Sigma \mathbf{S}_i\mathbf{S}_j$ is weakly ferromagnetic, with $J_{\rm iso}\approx 20$ K.[13] However, the very large temperature-independent width (for $T>100$ K) of $\Delta H\approx 1.8$ kOe suggests the presence of unusually large anisotropic corrections to $\mathcal{H}_{\rm iso}$ which are of the order of $\sim 10\%$ of $J_{\rm iso}$.[30] This strong anisotropic contribution to superexchange can be explained qualitatively as the result of the specific Cu-O bonding geometry involving two symmetric 90° Cu–O–Cu bonds which connect nearest-neighbor Cu sites. In this geometry the influence of spin-orbit coupling on the magnetic exchange between Cu^{2+} ions is found to be considerably enhanced.[44,45] Due to the substantial hole doping of the chains in the Sr-Ca system, the dominating exchange interaction occurs between *next-nearest*-neighbor Cu sites via an intermediate Zhang-Rice singlet. The drastic contrast between the very narrow ESR signal of $Sr_{14}Cu_{24}O_{41}$ and the very large width observed in $La_2Ca_{12}Cu_{24}O_{41}$ thus demonstrates that the anisotropy of the exchange coupling is very different for nearest-neighbor and next-nearest-neighbor couplings. In fact there is a certain similarity between the coupling via a Zhang-Rice singlet in the Sr-Ca system and the situation in a 180° Cu–O–Cu bond: in both cases the coupling strength is antiferromagnetic and large and shows a relatively small anisotropy due to the quenched orbital momentum of Cu^{2+}.

The additional increase of ΔH *below* 100 K with decreasing temperature in $La_2Ca_{12}Cu_{24}O_{41}$ shows that the system approaches long-range magnetic order at low temperatures, as discussed in Ref. 30. According to the analysis of $\chi_{\rm static}$ in Ref. 13, insulating $La_{14-x}Ca_xCu_{24}O_{41}$ is paramagnetic above 50 K, whereas at lower temperatures spin correlations grow and finally result in long-range AF order, which has been observed in $La_5Ca_9Cu_{24}O_{41}$ at $T_N\approx 10$ K.[46,47] Based on the magnetic-field dependence of the specific heat anomaly at the phase transition an Ising-like character of the chain magnetism has been suggested.[46] The increase of ΔH for temperatures larger than the magnetic ordering temperature is caused by short-range fluctuations of the staggered magnetization. These enhance the rate of the spin-spin relaxation $1/T_2$ and consequently broaden the ESR line additionally.[48]

The data of ΔH of $La_1Sr_{13}Cu_{24}O_{41}$ show an interesting mixture of the properties of the Sr-Ca system and the La-Ca system. The absolute value of ΔH of $La_1Sr_{13}Cu_{24}O_{41}$ is higher than observed in the former and lower than found in the latter. At high temperatures, it shows the same line broadening $\Delta H^*(T)$ induced by hole mobility as the Sr-Ca compounds, whereas at low temperatures it broadens additionally, thereby signaling the growth of short-range magnetic correlations as in the La-Ca samples.

2. Quasifree spins

The susceptibility data of Fig. 3 clearly indicate a crossover at about 25 K, below which the main contribution to both $\chi_{\rm stat}$ and $\chi_{\rm ESR}^{spin}$ stems from the $1/T$ Curie term of the quasifree spins. It is reasonable to assume that at low temperatures the ESR line of the quasifree spins has a width different from that of the response of the interacting spins which dominates at high temperatures. Therefore one can attribute the anomalies of ΔH at about 25 K to a corresponding crossover. In the crossover region we do not observe any significant distortion of the shape of the ESR spectrum since the resonance fields of the two contributions are rather similar. Whereas $x=0$ and 5 consistently show a rather small

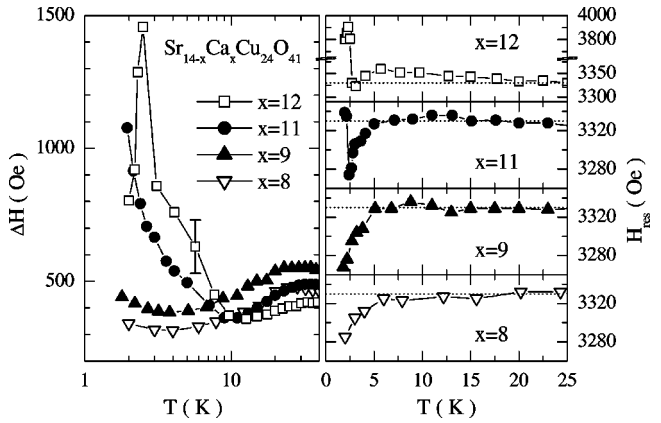

FIG. 5. Low-temperature behavior of the linewidth ΔH (left panel) and of the resonance field $H_{\rm res}$ (right panels) of $Sr_{14-x}Ca_xCu_{24}O_{41}$ for $x=8$, 9, 11, and 12. The magnetic field has been applied along the c axis. Note the different scale of the top right panel. Dotted lines are a guide to the eye and indicate $H_{\rm res}=3330$ Oe.

decrease of ΔH with decreasing T, we observe a pronounced upturn for $x=2$. Additional studies are required to clarify this discrepancy. The much stronger anomalies for larger values of x are discussed in the next section.

3. Magnetic order for large x

The low-temperature behavior of ΔH and $H_{\rm res}$ of the samples with $x\geqslant 8$ is shown in Fig. 5. Below 25 K the four samples with $x=8$, 9, 11, and 12 first show a decrease of ΔH with decreasing temperature, and then an *increase* at even lower temperatures. With increasing x the temperature at which ΔH acquires its minimum value increases from 3 to 13 K. At the same time, the low-temperature maximum value of ΔH increases as well, reaching $\Delta H\approx 1100$ Oe for $x=11$ and 1500 Oe for $x=12$. Finally, ΔH exhibits a sharp kink at $T=2.5$ K for $x=12$. Remarkably, this kink is accompanied by a dramatic shift of $H_{\rm res}$, which first drastically increases below 3 K and then exhibits a small kink at 2.3 K (see right panel of Fig. 5 and note the different scale of the top panel). Both anomalies clearly indicate a transition to a magnetically ordered state at 2.5 K for $x=12$. The cusp of ΔH at the ordering temperature is due to critical magnetic fluctuations which are strongest in the vicinity of the phase transition. The strong increase of $H_{\rm res}$ is typical for the transition to an antiferromagnetic state and indicates the development of a staggered internal magnetic field opposing the applied field. This is consistent with recent reports of antiferromagnetic order for $x=11.5$ and $x\geqslant 12.5$ (Refs. 26–28), where the ordered moments were found to reside mostly in the chains. Our ESR data demonstrate that the increase of the Ca content from $x=8$ to 11 continuously drives the system towards an antiferromagnetic instability. The slowing down of antiferromagnetic correlations above the ordering temperature[49] gives rise to critical broadening of the linewidth which is observed for all four samples with $x=8$, 9, 11, and 12. For $x=11$ the increase of ΔH is almost as large as for $x=12$, suggesting that magnetic order may occur for $x=11$ not too far below the lowest temperature that we have measured, 1.9 K. Note that this is confirmed by the temperature dependence of $H_{\rm res}$ for $x=11$, which shows a sudden increase at the lowest temperatures measured. However, from 5 to 2 K the resonance field $H_{\rm res}$ is *decreasing* for $x=8$, 9, and 11, which may imply the presence of competing *ferromagnetic* spin correlations in the system.

In our ESR data, magnetic correlations are confined to temperatures below 10 K, suggesting a low-energy scale for the magnetic exchange. In fact, small interdimer magnetic couplings of different signs along and across the chains are found in $Sr_{14}Cu_{24}O_{41}$ (Refs. 3–5). In the presence of charge order the much larger intradimer coupling across a Zhang-Rice singlet forces the system into a nonmagnetic ground state. The melting of charge order induced by Ca substitution destroys the dimerized state. The occurrence of long-range magnetic order is easily understood if for large x the system is described in terms of antiferromagnetic chains (see Ref. 23 and the discussion above). In this situation small interchain couplings stabilize a magnetically ordered state at low temperatures.

IV. CONCLUSIONS

In this work we have studied the electron spin resonance of the Cu^{2+} ions in the chains of intrinsically hole-doped single crystals of $Sr_{14-x}Ca_xCu_{24}O_{41}$ ($x=0$, 2, 5, 8, 9, 11, and 12) which contain six holes per formula unit. We compare the results with the ESR data of two single crystals of $La_1Sr_{13}Cu_{24}O_{41}$ and $La_2Ca_{12}Cu_{24}O_{41}$ in which the hole count is reduced to five and four, respectively. For small values of the Ca concentration x the ESR measurement of $Sr_{14-x}Ca_xCu_{24}O_{41}$ probes the spin dimers above 25 K. We find that the Cu-spin relaxation is appreciably influenced by the charge dynamics in the chains, resulting in a strong temperature dependence of the ESR linewidth ΔH above a characteristic temperature T^*. The crossover to a nearly temperature-independent width ΔH_0 below T^* is identified with the onset of charge order in the chains. With increasing x this crossover shifts from about 200 K in $Sr_{14}Cu_{24}O_{41}$ to ~ 80 K for $x=5$, indicating a rapid destruction of charge order. Remarkably, the spin relaxation is strongly temperature dependent even at high Ca values like $x=11$ and 12, suggesting the presence of a substantial amount of holes in the chains. At the same time, the spin relaxation of $La_1Sr_{13}Cu_{24}O_{41}$ containing five holes per formula unit in the chains is rather similar to the one of $Sr_{14-x}Ca_xCu_{24}O_{41}$ for large x at high temperatures. A further reduction of the hole count form five to four as in $La_2Ca_{12}Cu_{24}O_{41}$ results in a very different ESR linewidth. These results give an upper border of one hole being transferred from the chains to the ladders upon Ca substitution of $Sr_{14-x}Ca_xCu_{24}O_{41}$. A certain transfer of holes explains the increase of ΔH_0 with increasing x: its main impact on the ESR linewidth is related to the enhancement of the probability of having two spins on neighboring sites, resulting in both a strongly enhanced anisotropy and a considerably reduced exchange narrowing. At the same time, a reduced hole count destroys the charge order and therefore gives rise to locally different dipolar fields,

again resulting in an enhanced linewidth. For $x \geqslant 8$ the low-temperature ESR signal experiences critical broadening and a strong shift of the resonance field, giving evidence for a continuous crossover from the spin dimerized to an antiferromagnetically ordered ground state with increasing x, i.e., for large x the system is better described in terms of weakly interacting antiferromagnetic chains.

ACKNOWLEDGMENTS

We gratefully acknowledge useful discussions with B. Keimer, G. A. Sawatzky, and E. Müller-Hartmann. This work was supported by the Deutsche Forschungsgemeinschaft through SFB 341 and SP 1073 and by the DAAD in the frame of PROCOPE.

*On leave from Kazan Physical Technical Institute, Russian Academy of Sciences, 420111 Kazan, Russia.

†Present address: 2. Physikalisches Institut, RWTH Aachen, D-52056 Aachen, Germany.

[1] For a review, see E. Dagotto, Rep. Prog. Phys. **62**, 1525 (1999).

[2] E.M. McCarron III, M.A. Subramanian, J.C. Calabrese, and R.L. Harlow, Mater. Res. Bull. **23**, 1355 (1998); T. Siegrist, L.F. Schneemeyer, S.A. Sunshine, J.V. Waszczak, and R.S. Roth, *ibid.* **23**, 1429 (1998).

[3] R.G. Eccleston, M. Uehara, J. Akimitsu, H. Eisaki, N. Motoyama, and S. Uchida, Phys. Rev. Lett. **81**, 1702 (1998).

[4] L.P. Regnault, J.P. Boucher, H. Moudden, J.E. Lorenzo, A. Hiess, U. Ammerahl, G. Dhalenne, and A. Revcolevschi, Phys. Rev. B **59**, 1055 (1999).

[5] M. Matsuda, T. Yosihama, K. Kakurai, and G. Shirane, Phys. Rev. B **59**, 1060 (1999).

[6] Y. Mizuno, T. Tohyama, and S. Maekawa, J. Phys. Soc. Jpn. **66**, 937 (1997).

[7] N. Nücker, M. Merz, C.A. Kuntscher, S. Gerhold, S. Schuppler, R. Neudert, M.S. Golden, J. Fink, D. Schild, S. Stadler, V. Chakarian, J. Freeland, Y.U. Idzerda, K. Conder, M. Uehara, T. Nagata, J. Goto, J. Akimitsu, N. Motoyama, H. Eisaki, S. Uchida, U. Ammerahl, and A. Revcolevschi, Phys. Rev. B **62**, 14 384 (2000).

[8] K. Magishi, S. Matsumoto, Y. Kitaoka, K. Ishida, K. Asayama, M. Uehara, T. Nagata, and J. Akimitsu, Phys. Rev. B **57**, 11 533 (1998).

[9] K. Kumagai, S. Tsuji, M. Kato, and Y. Koike, Phys. Rev. Lett. **78**, 1992 (1997).

[10] R.S. Eccleston, M. Azuma, and M. Takano, Phys. Rev. B **53**, 14 721 (1996).

[11] M. Matsuda, K. Katsumata, H. Eisaki, N. Motoyama, S. Uchida, S.M. Shapiro, and G. Shirane, Phys. Rev. B **54**, 12 199 (1996).

[12] U. Ammerahl, B. Büchner, L. Colonescu, R. Gross, and A. Revcolevschi, Phys. Rev. B **62**, 8630 (2000).

[13] S.A. Carter, B. Batlogg, R.J. Cava, J.J. Krajewski, W.F. Peck, Jr., and T.M. Rice, Phys. Rev. Lett. **77**, 1378 (1996).

[14] D.E. Cox, T. Iglesias, K. Hirota, G. Shirane, M. Matsuda, N. Motoyama, H. Eisaki, and S. Uchida, Phys. Rev. B **57**, 10 750 (1998).

[15] F.C. Zhang and T.M. Rice, Phys. Rev. B **37**, 3759 (1988).

[16] M. Matsuda and K. Katsumata, Phys. Rev. B **53**, 12 201 (1996).

[17] N. Motoyama, T. Osafune, T. Kakeshita, H. Eisaki, and S. Uchida, Phys. Rev. B **55**, 3386 (1997).

[18] M. Uehara, T. Nagata, J. Akimotsu, H. Takahashi, N. Môri, and K. Kinoshita, J. Phys. Soc. Jpn. **65**, 2764 (1996).

[19] T. Nagata, M. Uehara, J. Goto, J. Akimitsu, N. Motoyama, H. Eisaki, S. Uchida, H. Takahashi, T. Nakanishi, and N. Môri, Phys. Rev. Lett. **81**, 1090 (1998).

[20] T.M. Rice, S. Goapalan, and M. Sigrist, Europhys. Lett. **23**, 445 (1993).

[21] T. Osafune, N. Motoyama, H. Eisaki, and S. Uchida, Phys. Rev. Lett. **78**, 1980 (1997).

[22] S. Katano, T. Nagata, J. Akimitsu, M. Nishi, and K. Kakurai, Phys. Rev. Lett. **82**, 636 (1999).

[23] U. Ammerahl, Ph.D. thesis, University of Cologne, 2000; U. Ammerahl, R. Klingeler, B. Büchner, M. Hücker, and A. Revcolevschi (unpublished).

[24] The susceptibility shows a maximum at $T_{\max}^{\text{chain}} \simeq 0.641\ J/k_B$ (Ref. 25) for an AF chain and at $T_{\max}^{\text{dimer}} \simeq 0.624\ J/k_B$ (Ref. 23) for independent dimers.

[25] D.C. Johnston, R.K. Kremer, M. Troyer, X. Wang, A. Klümper, S.L. Bud'ko, A.F. Panchula, and P.C. Canfield, Phys. Rev. B **61**, 9558 (2000).

[26] M. Isobe, Y. Uchida, and E. Takayama-Miromachi, Phys. Rev. B **59**, 8703 (1999).

[27] S. Ohsugi, K. Magishi, S. Matsumoto, Y. Kitaoka, T. Nagata, and J. Akimitsu, Phys. Rev. Lett. **82**, 4715 (1999).

[28] T. Nagata, H. Fujino, J. Akimitsu, M. Nishi, K. Kakurai, S. Katano, M. Hiroi, M. Sera, and N. Kobayashi, J. Phys. Soc. Jpn. **68**, 2206 (1999).

[29] D. König, U. Löw, S. Schmidt, H. Schwenk, M. Sieling, W. Palme, B. Wolf, G. Bruls, B. Lüthi, M. Matsuda, and K. Katsumata, Physica B **237-238**, 117 (1997).

[30] V. Kataev, K.-Y. Choi, M. Grüninger, U. Ammerahl, B. Büchner, A. Freimuth, and A. Revcolevschi, Phys. Rev. Lett. **86**, 2882 (2001).

[31] U. Ammerahl, G. Dhalenne, A. Revcolevschi, J. Berthon, and H. Moudden, J. Cryst. Growth **193**, 55 (1998); U. Ammerahl and A. Revcolevschi, *ibid.* **197**, 825 (1999).

[32] A. Abragam and B. Bleaney, *Electron Paramagnetic Resonance of Transition Ions* (Clarendon, Oxford, 1970).

[33] In the case of antiferromagnetic coupling, the number of spins of a fragment should be odd, see J.C. Bonner and M.E. Fischer, Phys. Rev. **135**, A640 (1964).

[34] D.C. Johnston, M. Troyer, S. Miyahara, D. Lidsky, K. Ueda, M. Azuma, Z. Hiroi, M. Takano, M. Isobe, Y. Ueda, M.A. Korotin, V.I. Anisimov, A.V. Mahajan, and L.L. Miller, cond-mat/0001147 (unpublished).

[35] An analysis of neutron scattering data under the assumption that J_{leg} and J_{rung} are the only relevant parameters yields $J_{\text{leg}} \approx 1500$ K and $J_{\text{rung}}/J_{\text{leg}} \approx 0.55$ (Ref. 3), but more recently it has been shown that a more consistent description is obtained by using $J_{\text{leg}} \approx 1300$ K, $J_{\text{rung}}/J_{\text{leg}} = 1$ and a four-spin cyclic exchange $J_{\text{ring}} \approx 190$ K (Ref. 36).

[36] M. Matsuda, K. Katsumata, R.S. Eccleston, S. Brehmer, and H.-J. Mikeska, Phys. Rev. B **62**, 8903 (2000).

[37] A. Klümper, Eur. Phys. J. B **5**, 677 (1998).

[38] The contribution to the linewidth ΔH_0 due to symmetric aniso-

tropic exchange $\mathcal{H}' = \Sigma S_i A S_j$ is set by the second moment of the resonance line $M_2 = \langle [\mathcal{H}'(0), M_+(0)]^2 \rangle / \hbar^2 \langle M_+ M_- \rangle$ (see, e.g., Ref. 39). Here, the numerator yields four-spin correlation functions at time $t=0$, and M_+ and M_- are the transverse magnetizations, with $\langle M_+ M_- \rangle = 2 k_B T \chi_{\rm stat}(T)$. In the high-temperature limit, i.e., $k_B T \gg J_{\rm iso}$, the moment M_2 acquires a temperature dependence if the static susceptibility $\chi_{\rm stat}(T)$ deviates from the Curie law, but is temperature independent if $\chi_{\rm stat}(T)$ obeys the $1/T$ behavior (Ref. 40). However, if temperature is reduced to values comparable to the energy scale of the *isotropic* exchange $J_{\rm iso}$, the moment M_2 does *not* exhibit a strong temperature dependence, even if $\chi_{\rm stat}$ deviates from $1/T$ (see, e.g., Refs. 41 and 42). We therefore assume M_2 and ΔH_0 to be constant. This assumption is justified in particular by the data of $Sr_{14}Cu_{24}O_{41}$, for which the ESR signal shows a constant width between 30 and ≈ 180 K, even though χ_{stat} considerably deviates from the Curie law in a large part of this temperature range (see discussion below).

[39] R. Kubo and K. Tomita, J. Phys. Soc. Jpn. **9**, 888 (1954).

[40] D.L. Huber, G. Alejandro, A. Caneiro, M.T. Causa, F. Prado, M. Tovar, and S.B. Oseroff, Phys. Rev. B **60**, 12 155 (1999).

[41] Z.G. Soos, K.T. McGregor, T.T.P. Cheung, and A.J. Silverstein, Phys. Rev. B **16**, 3036 (1977).

[42] I. Yamada, H. Fujii, and M. Hikada, J. Phys.: Condens. Matter **1**, 3397 (1989).

[43] M. Takigawa, N. Motoyama, H. Eisaki, and S. Uchida, Phys. Rev. B **57**, 1124 (1998).

[44] V.Yu. Yushankhai, and R. Hayn, Europhys. Lett. **47**, 116 (1999).

[45] S. Tornow, O. Entin-Wohlman, and A. Aharony, Phys. Rev. B **60**, 10 206 (1999).

[46] U. Ammerahl, B. Büchner, C. Kerpen, R. Gross, and A. Revcolevschi, Phys. Rev. B **62**, R3592 (2000).

[47] M. Matsuda, K.M. Kojima, Y.J. Uemura, J.L. Zaretsky, K. Nakajima, K. Kakurai, T. Yokoo, S.M. Shapiro, and G. Shirane, Phys. Rev. B **57**, 11 467 (1998).

[48] D.L. Huber, Phys. Rev. B **6**, 3180 (1972).

[49] H. Benner and J. P. Boucher, in *Magnetic Properties of Layered Transition Metal Compounds*, edited by L. J. de Jongh (Kluwer Academic, Boston, 1990), p. 323.